INJECTION IN THE VICKSI CYCLOTRON

S. Lindbäck and H. Lindqvist
Instrument AB Scanditronix, Uppsala, Sweden

1. Introduction

The heavy ion accelerator combination VICKSI[1-3] consists of a 6MV-CN-Van de Graaff accelerator serving as injector for a separated sector cyclotron being built by Scanditronix, Sweden. The injector which is undergoing a major reconstruction will produce multiply charged ions ($q \leq 3$) ranging from protons to argon. After stripping, the ions are injected into the cyclotron and accelerated up to a maximum final energy of 120 q^2/m MeV, variable by a factor of 10. Acceleration is done via two symmetrical 100 kV, 36^0 dees tunable from 8 to 20 MHz.

The beam transfer system between the two accelerators [4] consists of two bunchers, a combined gas or carbon foil stripper, conventional bending magnets and quadrupoles. The system has been designed to yield good flexibility regarding the matching of dispersion and emittances.

Fig. 1 shows a plan view of the two accelerators and the beam transfer line. Beam emittances of about 10π mm x mrad are expected in both planes after stripping and beam currents ranging from 100 particle-nanoamperes for heavy ions to 10 microamperes for protons. The bunching system compresses 60 % of the d.c.-beam into a phase interval of 6^0 before acceleration starts in the cyclotron. The momentum spread in the useful part of the beam is calculated to lie within ± 0.25 %.

2. Configuration

We have chosen radial injection as being more simple and straightforward than vertical injection. Fig. 2 shows the adopted layout. The beam is injected via a dee-free valley into a 7^0 window frame magnet (I_1) followed by an 86^0 homogenous field bending magnet (I_2). That element bends the beam into a

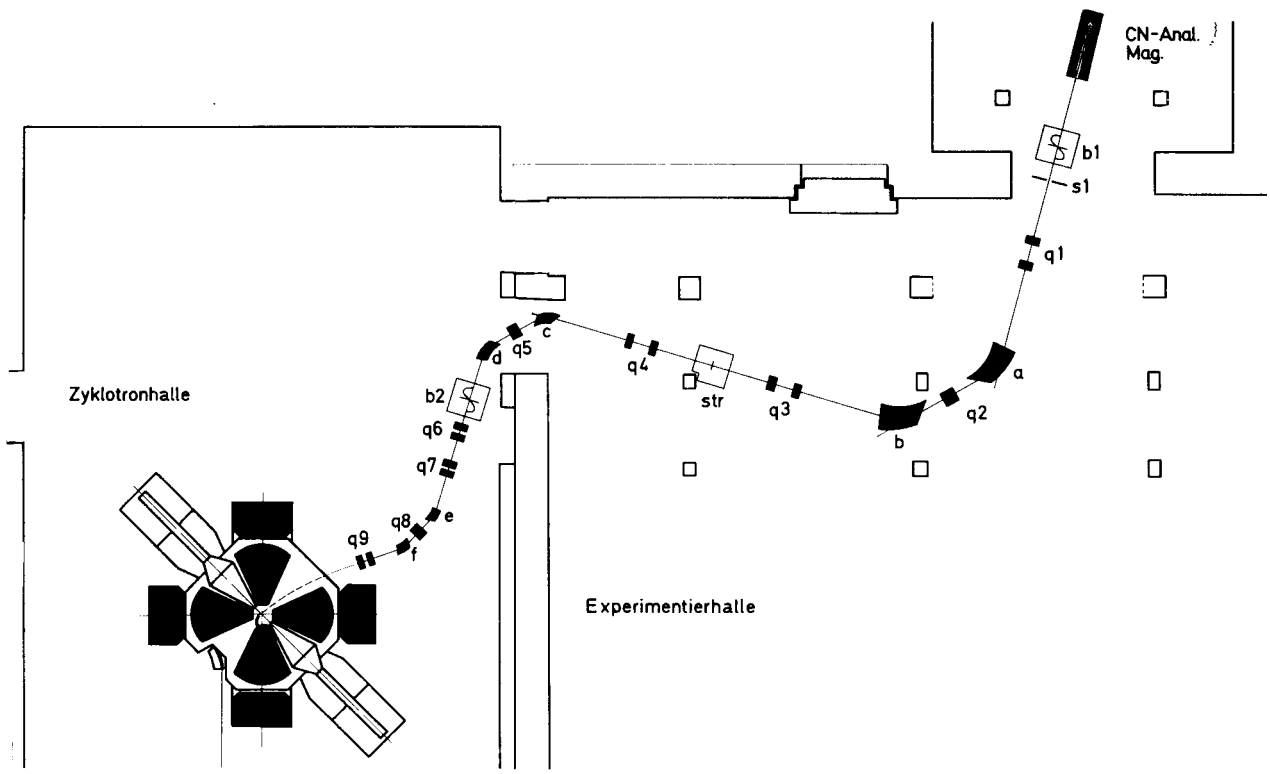

Fig. 1 Layout of injector, beam transfer system and cyclotron

Proc. 7th Int. Conf. on Cyclotrons and their Applications (Birkhäuser, Basel, 1975), p. 226-230

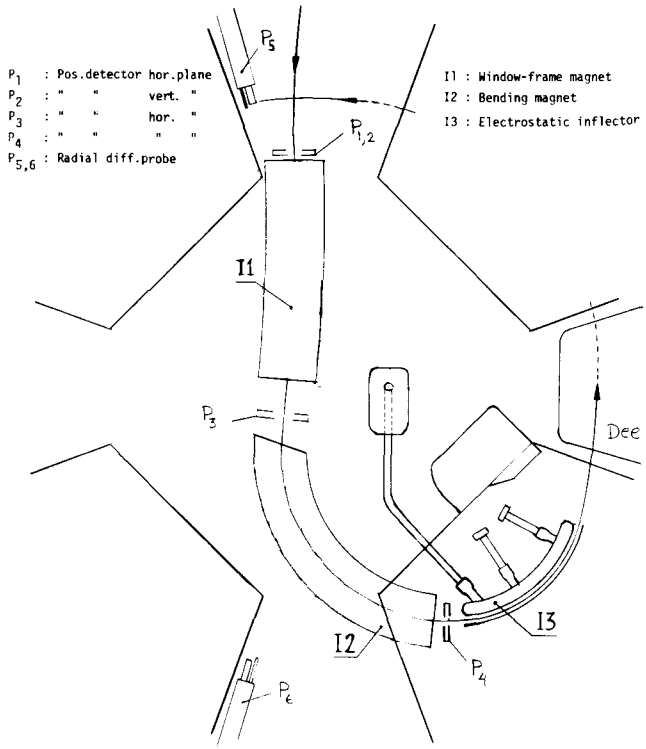

Fig. 2 Schematical layout of central region showing injection elements and diagnostic probes

sector nose where a 27 cm long electrostatic inflector (I_3) brings the beam onto the accelerated equilibrium orbit by adding 30 % bending power to the sector field. This corresponds to a maximum field strength of 110 kV/cm for $^3He^{2+}$ ions and about 30 kV/cm for $^{40}Ar^{9+}$ ions.

I_2 is essentially passive the flux being provided equally by all four sectors via two horizontal floating iron plates. A small coil on the yoke will be used to compensate for saturation effects and for beam alignment purposes. The pole gap of I_2 is 15 mm and the pole width 80 mm, which ensures sufficient field homogenity along the centre line. Both I_1 and I_2 have been measured and shimmed in a half scale sector model and full scale versions have now been manufactured.

A model of I_3 has been successfully tested in full scale. The anti-septum will be made of stainless steel supported by Al_2O_3 insulators and the septum of copper. The vertical distance between the spark plates is 40 mm and between anti-septum and spark plate 8 mm. The horizontal aperture is 7 mm.

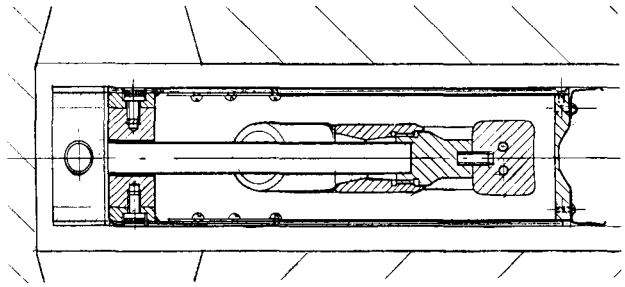

Fig. 3 Cross-section of electrostatic inflector I_3

Fig. 3 shows the cross-section of I_3. The anti-septum has been designed to minimize non-linear vertical components of the electric field in the volume occupied by the beam. This was done using a trial-error method with the aid of a programme solving the Laplace equation [5].

The position of the electrostatic inflector I_3 will be remotely controlled while I_1 and I_2 are fixed. We will try to minimize the transverse movements of I_3 to a few millimeters, in order to reduce the mechanical and electrical stresses on the insulators and H.V. feed line. This is possible, inspite of the variety of ions to be injected, thanks to the inflector being placed in the sector gap. This is the place where the difference in angle of accelerated equilibrium orbits gets smallest when comparing ions of maximum and minimum turn separation.

Fig. 4 illustrates this for $^3He^{2+}$ and $^{40}Ar^{9+}$ ions. The energies are chosen so that the trajectories

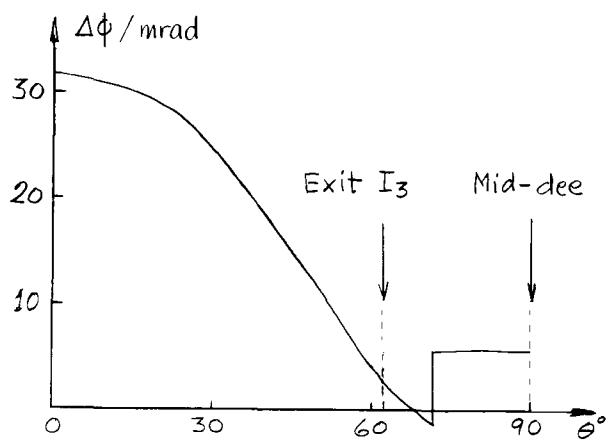

Fig. 4 Difference in beam angle ($\Delta\phi$) vs azimuth (θ) between $^{40}Ar^{9+}$ and $^3He^{2+}$ ions.

cross over at the exit of I_3. Placing the inflector in the valley at $\theta = 0^o$ (as would be done in one of the alternative radial injection schemes) would require deflector movements of about 2^o.

From fig. 4 we find that the difference in beam angle at the exit of I_3 ($\theta = 62^o$) is about 3 milliradians. For such small angles the inflector voltage can be adjusted to give practically constant orbit geometry through the inflector.

3. Dispersion and emittance matching

The beam matching procedure has been carried out using the programme TRANSPORT[6]. The transfer matrix from the entrance of the cyclotron to the mid-dee valley line was found on computer by tracking orbits in the actual measured field. The elements I_2 and I_3 were represented analytically. All optimizations have been done in the reverse beam direction, i.e. starting in the dee valley and ending at the entrance of bending magnet e (see fig. 1).

The (r, p_r)-relation to be fulfilled by off-momentum particles have been found by tracking accelerated equilibrium orbits of different energy at small radii. At the exit of I_3 this relation leads to the following values for the dispersion elements R_{16} and R_{26} of the first order transfer matrix R.

$$\begin{pmatrix} R_{16} \\ R_{26} \end{pmatrix} = \begin{matrix} -0.4 \text{ cm/\%} \\ +0.44 \text{ mrad/\%} \end{matrix}$$

where momentum deviation is given in percent (nomenclature as in TRANSPORT). Downstream in the middle of the dee valley $R_{16} = -0.4$, $R_{26} \approx 0$ and the eigenellipses are both upright.

Three parameters are available for matching to the desired dispersion relation (R_{16}, R_{26}), viz. the quadrupole singlet q8 and the doublet q9 (fig. 1). For this matching only two parameters are required. The third one can be used to limit the vertical beam size in the bending magnets e, f and to give the beam ellipses a favourable shape at the entrance of e.

The dashed area in fig. 5 indicates the flexibility of the system regarding the choice of R_{16} and R_{26}. Within this area matching of the transverse emittances has also been successfully performed.

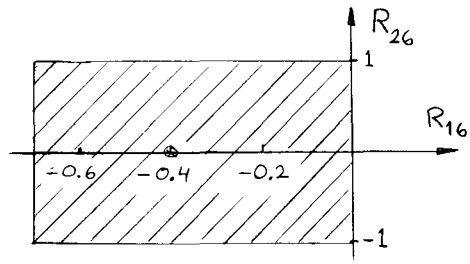

Fig. 5 Dashed region shows achievable combinations of dispersion elements R_{16} and R_{26} in middle of dee valley.

The emittances are matched to the eigenellipses of the cyclotron. In the mid-valleys these are both upright with widths of 1.7 mm horizontally and 2.5 mm vertically. The beam optical system can provide somewhat narrower or broader ellipses (<20 % variation of the width of the ellipse) but to achieve ellipses substantially different from the eigenellipses would require a modification of the entrance angle of I_2 (now -17.5^o) in order to better share the increased beam size outside the cyclotron between the two planes of motion.

The system has nominally been designed to yield a longitudinal focus in the mid-dee valley, but this can be modified to other longitudinal ellipse orientations by means of the voltage in the last buncher and, in the case there is no time focus at the stripper also by using the preceeding buncher. The final choice will be based on results from accelerated beam studies, considering oscillations in phase width, the possible use of phase slits, energy spread in the beam, single turn extraction etc.

Fig. 6 gives the beam envelopes (half widths) for the transverse motion from the entrance of the bending magnet e to the middle of the first dee. Outside the cyclotron beam half widths of 2.5 - 3 cm occur but in the central region of the cyclotron the corresponding values are only 2 - 3 mm.

4. Beam diagnostics and alignment

The transverse emittances and the time-momentum correlation of the beam will be measured by two

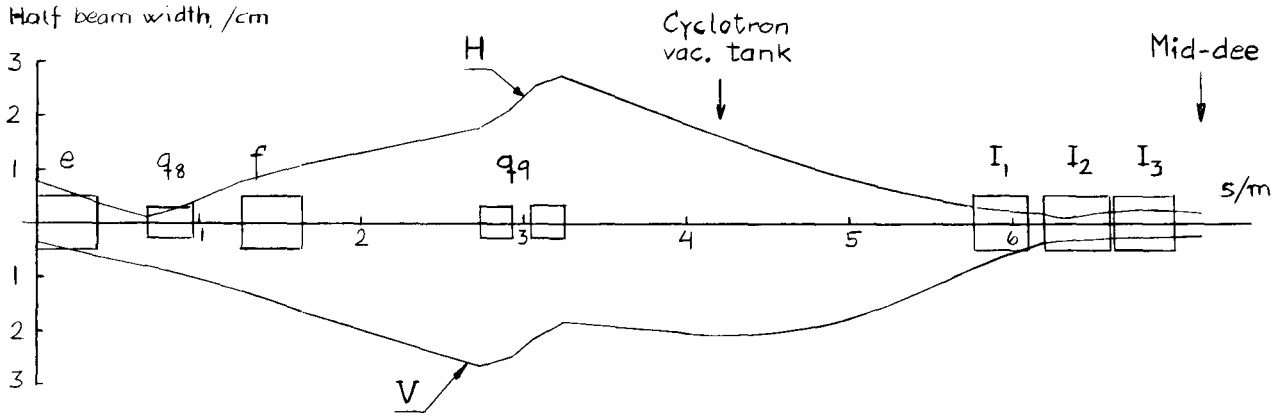

Fig. 6 Beam envelope in horizontal (H) and vertical (V) plane as a function of system length (s).

permanently installed devices immediately after the bending magnet f as explained in ref. 4. Before the beam enters the cyclotron a rotating beam scanner and Faraday cup give beam position and current.

Fig. 2 shows the layout of diagnostic probes used for the injection. By means of a small combined horizontal and vertical steering magnet the beam will be swept horizontally and vertically over a fixed detector $P_{1,2}$ placed at the entrance of I_1. The detector measures total beam current, beam shape and position in both planes as a function of steering currents (important for beam alignment).

Two similar fixed detectors P_3 and P_4 at the entrance of I_2 and I_3 will be used for alignment of the beam in the horizontal plane. This is done by sweeping the beam by means of I_1 and the auxiliary coil of I_2, respectively. P_4 is mounted on the inflector assembly and helps protect the anti-septum from the beam. Just prior to P_4 the beam has a horizontal waist and a lateral dispersion of 3.8 mm/%. By choosing an aperture on P_4 of 4 mm all particles with $dp/p > 1$ % will be stopped.

The transmission through I_3 will be checked by observing the beam intensity on the radial (differential) probe P_5. This probe plus one similar P_6 will be used for diagnostics on the accelerated beam. Corrections in beam alignment can be done by adjusting two or more of the injection elements. As an example, a change of 1 milliradian in the steering magnet and of 1 % in the field of I_2 implies -2 mm and -10 milliradians, respectively, in beam position and angle in the middle of the dee valley. The position of I_3 and the dee voltage give two further parameters which may be used for beam centering.

5. Acknowledgements

The authors wish to express their thanks to Dr. G. Hinderer for many helpful discussions.

References

1. VICKSI-proposal, HMI-report B-118 (1972)

2. B. Efken et al. 6th International Cyclotron Conference, Vancouver 1972. A.I.P. Proceedings No. 9, p. 63

3. K.H. Maier, VICKSI Status Report, these proceedings

4. G. Hinderer, K.H. Maier, The beam-matching system between pre- and main-accelerator for the Van de Graaff-cyclotron combination VICKSI. 6th Particle Accelerator Conference, Washington D.C. (1975)

5. U. Janetzki, HMI, Private communication

6. K.L. Brown, D.C. Carey, Ch. Iselin and F. Rothacker, TRANSPORT, a computer program for designing charged particle beam transport systems, CERN 73-16 (1973)

DISCUSSION

G.H. MACKENZIE: How thick are your solid stripper foils and how much does multiple scattering contribute to your emittance?

S.R. LINDBÄCK: If you do not mind I suggest that Dr. Maier from Berlin answers this question.

K.H. MAIER: 2-3 $\mu g/cm^2$ are necessary to reach the equilibrium charge state distribution. Our trials have been with 5-10 $\mu g/cm^2$ foils. For the final stripper arrangement, the emittance will increase from just above 5π mm × mrad to just below 10π mm × mrad.

H.G. BLOSSER: If I understand correctly, the steering elements occur before the electrostatic inflector and the inflector is fixed in position.

S.R. LINDBÄCK: Yes, the corrections occur before, but the inflector will be remotely movable. We will, however, try hard to minimize the needs for movements in order to reduce stresses on support insulators and feed line.

S. ADAM: Did you test the voltage-holding capability in the magnetic field?

S.R. LINDBÄCK: Yes, we have carried out an extensive test programme in a test magnet at rather realistic conditions.

G. DUTTO: Do you plan to measure the centre region B_r component on the full scale magnets?

S.R. LINDBÄCK: We have not yet taken a final decision. Our ν_z starts at about 0.65 which is far from resonances sensitive to B_r components, so we have given such a measurement somewhat lower priority in view of our tight time schedule.